JOURNAL OF MORPHOLOGY 277:766–775 (2016)

Adaptive Evolution of a Derived Radius Morphology in Manakins (Aves, Pipridae) to Support Acrobatic Display Behavior

Anthony Friscia,[1] Gloria D. Sanin,[2] Willow R. Lindsay,[3,4] Lainy B. Day,[4] Barney A. Schlinger,[1,5,6,7] Josh Tan,[8] and Matthew J. Fuxjager[2]*

[1]*Department of Integrative Biology and Physiology, University of California, Los Angeles, Los Angeles, California 90095*
[2]*Department of Biology, Wake Forest University, Winston-Salem, North Carolina 27109*
[3]*Department of Biological and Environmental Sciences, Gothenburg University, Gothenburg, Sweden*
[4]*Department of Biology, University of Mississippi, University, Mississippi 38677*
[5]*Laboratory of Neuroendocrinology, University of California, Los Angeles, California 90095*
[6]*Department of Ecology and Evolutionary Biology, University of California, Los Angeles, California 90095*
[7]*Smithsonian Tropical Research Institute, Balboa, Ancon, Panama*
[8]*Department of Radiology, Wake Forest University School of Medicine, Winston-Salem, North Carolina 27157*

ABSTRACT The morphology of the avian skeleton is often studied in the context of adaptations for powered flight. The effects of other evolutionary forces, such as sexual selection, on avian skeletal design are unclear, even though birds produce diverse behaviors that undoubtedly require a variety of osteological modifications. Here, we investigate this issue in a family of passerine birds called manakins (Pipridae), which have evolved physically unusual and elaborate courtship displays. We report that, in species within the genus *Manacus*, the shaft of the radius is heavily flattened and shows substantial solidification. Past work anecdotally notes this morphology and attributes it to the species' ability to hit their wings together above their heads to produce loud mechanical sonations. Our results show that this feature is unique to *Manacus* compared to the other species in our study, including a variety of taxa that produce other sonations through alternate wing mechanisms. At the same time, our data reveal striking similarities across species in total radius volume and solidification. Together, this suggests that supposedly adaptive alterations in radial morphology occur within a conserved framework of a set radius volume and solidness, which in turn is likely determined by natural selection. Further allometric analyses imply that the radius is less constrained by body size and the structural demands that underlie powered flight, compared to other forelimb bones that are mostly unmodified across taxa. These results are consistent with the idea that the radius is more susceptible to selective modification by sexual selection. Overall, this study provides some of the first insight into the osteological evolution of passerine birds, as well as the way in which opposing selective forces can shape skeletal design in these species. J. Morphol. 277:766–775, 2016. © 2016 Wiley Periodicals, Inc.

KEY WORDS: avian skeleton; sexual selection; courtship display; manakin; passerine bird

INTRODUCTION

Skeletal systems in many volant birds are under strong positive selection for efficient bone design to reduce costs associated with generating lift during flight (Fedducia, 1996; Gill, 2007; Dumont, 2010). In this regard, the avian skeleton reflects an exquisite balance between osteological strength and lightweight proficiency necessary to economically support everyday life and powered locomotion. However, in some avian clades, skeletal design varies in response to selection for other physiological and behavioral traits or features that are not related to flight (Weston et al., 2007; Hone et al., 2011; Bostwick et al., 2012; Olson and Turvey, 2013; Naish and Perron, 2014). The nature of this osteological variation is seldom explored in extant birds, even though many avian species have evolved unique behavioral repertoires that otherwise require unusual and complex body and limb movements (Wallace, 1869; Beehler and Pruett-Jones, 1983; Prum, 1990, 1998; Jaramillo and Burke, 1999; Clifton et al., 2015).

Recent work in avian osteology highlights the different ways that bone morphology is shaped, not only by selection for flight, but also by a

Additional Supporting Information may be found in the online version of this article.

*Correspondence to: Matthew J. Fuxjager; Department of Biology, Wake Forest University, Winston-Salem, NC, 27109.
Email: mfoxhunter@gmail.com

Received 23 January 2016; Revised 18 February 2016; Accepted 27 February 2016.

Published online 29 March 2016 in Wiley Online Library (wileyonlinelibrary.com).
DOI 10.1002/jmor.20534

variety of other functional factors. Some diving birds, for example, maintain certain limb bones that are heavily ossified to serve as ballasts (Currey and Alexander, 1985; Habib and Ruff, 2008). Another recent study in club-winged manakins (*Machaeropterus deliciosus*) shows that individuals have enlarged and solidified ulnas (Bostwick et al., 2012), compared to other manakin species. These derived features of this specific forearm bone are thought to support the performance of an elaborate wing maneuver that is part of a courtship display. Thus, sexual selection is thought to influence this bird's ulna morphology by countering presumed effects of natural selection for an efficient forearm skeleton that supports flight. However, additional examination of this hypothesis is warranted. For example, this study does not look at whether related congeners show a similarly derived ulna. This work also does not address whether ulna solidness occurs throughout the entire bone, or whether solidness is found only within a particular region of the bone. Furthermore, neither this work in club-winged manakins, nor work in any other passerine species of which we are aware, examines allometric relationships between body size and features of the wing skeletal structure. Therefore, we have little insight into the basic morphological properties that might otherwise constrain avian skeletal design, particularly in terms of small birds like manakins. In this regard, it remains unclear how the wing bones might evolve to support complex and acrobatic avian displays.

The main goal of our study is to examine variation in wing bone morphology among a number of manakins that use their forelimbs to perform different types of physical display behavior. Yet, in contrast to the work of Bostwick et al. (2012) on the ulna of the club-winged manakin, our current study focuses on a different forearm bone in a separate manakin species; namely, we study the radius of the golden-collared manakin (*Manacus vitellinus*). Males of this species court potential mates by performing a behavioral display that includes the production of mechanical, firecracker-like wing-snaps (Fusani et al., 2007; Barske et al., 2011; Fuxjager et al., 2013; Barske et al., 2014). To produce this signal, males are thought to rapidly hit their wings together above their back (Fusani et al., 2014; Fusani et al., 2007; Schlinger et al., 2013; Schlinger et al., 2008), and prior work suggests that this bird maintains a derived radius morphology that accommodates this percussive sound-making ability (Friscia and Schlinger, 2012; Bodony et al., in press). Thus, we examine the forearm skeleton (including the radius, ulna, and humerus) in the golden-collared manakin, and we compare our findings to a variety of other manakin and passerine species. Foremost among these other birds is the white-collared manakin (*Manacus candei*), a congener of the golden-collared manakin that also produces a wing-snap (Bostwick and Prum, 2003). Likewise, we compare our findings to additional manakins that produce sonations through wing movements that are different from the species within the genus *Manacus*. These include the red-capped manakin (*Ceratopipra mentalis*), which produces wing sonations by slapping and rubbing its wings against its body (Bostwick and Prum, 2003), as well as the white-ruffed manakin (*Corapipo altera*) and lance-tailed manakin (*Chiroxiphia lanceolata*), both of which produce dramatic flight routines that involve low amplitude sonations from wing movements (Prum, 1998; Rosselli et al., 2002; DuVal, 2007). Although the exact mechanism for wing-sonation in these other species has not been determined, they do not appear to be created with the same type of behind-the-back wing movement or with the same percussive force as the two *Manacus*. Finally, as non-manakin out-groups, we include the spangled cotinga (*Cotinga cayana*), ochre-bellied flycatcher (*Mionectes oleaginous*), and Say's phoebe (*Sayornis saya*). Both the spangled cotinga and ochre-bellied flycatcher produce flight displays that are extremely modest, compared to the manakins (Westcott and Smith, 1994; Chaves, 2001), whereas the Say's phoebe produces little in terms of physical display behavior (Schukman and Wolf, 1998).

We analyze the deep architectural features of these birds' wing bones using micro-computer tomography (micro-CT). If derived radius morphology is an adaptation that underlies adaptive wing-snapping, then we expect to find it in both golden-collared and white-collared manakins. We do not expect to find such morphology in the other species, given that they either produce wing sonations that rely on alternate forelimb kinematics, or do not produce wing-snaps at all. With the species of *Manacus*, we expect to observe modifications in shape and solidness (percent ossified volume) along the part of the bone that is thought to constitute the wing's percussive element. Such results have the potential to reveal how such osteological modifications are balanced with other traits, such as total bone volume. In this regard, we predict that most elements of bone design are conserved through natural selection for locomotory performance (flight).

METHODS

Specimen Collection and Preservation

Details regarding the specimens we used in this study are outlined in Table 1. Five of these species were manakins (Pipridae), whereas three were non-manakin out-groups (one cotinga, one tyrant flycatcher, and one phoebe). Specimens were wild-caught individuals, with the exception of the cotinga and the phoebe, which were disarticulated osteological museum specimens. The wild caught birds were adult males in reproductive condition that were trapped passively (i.e., with no stimulus to lure birds into the net) using mist-nets in Panama. The golden-collared, red-capped, and lance-tailed manakins were collected in the region surrounding the township of Gamboa, Panama province (79°41′W, 9°07′N). The white-ruffed manakin was collected in

TABLE 1. Specimens used for analyses.

Species	Specimen ID	Sample size (n) for MicroCT scans[a]	Sample size (n) for manual morphometric comparisons[a]
Golden-collared manakin (*Manacus vitellinus* (Gould, 1843))	Wild-caught preserved specimen	1	3
White-collared manakin (*Manacus candei* (Parzudaki, 1841))	Wild-caught preserved specimen	1	N/A
Lance-tailed manakin (*Chiroxiphia lanceolata* (Wagler, 1830))	Wild-caught preserved specimen	1	N/A
Red-capped manakin (*Ceratopipra mentalis* (Sclater, 1857))	Wild-caught preserved specimen	1	3
White-ruffed manakin (*Corapipo altera* (Hellmayr, 1906))	Wild-caught preserved specimen	1	N/A
Spangled cotinga (*Cotinga cayana* (Linnaeus, 1766))	NHM 114812	1	N/A
Ochre-bellied flycatcher (*Mionectes oleaginous* (Lichtenstein, 1823))	Wild-caught preserved specimen	N/A	3
Say's phoebe (*Sayornis saya* (Bonaparte, 1825))	NHM 115671	N/A	1

[a]N/A indicates that the species was not included in the given analysis.

Parque Omar Torrijos, Coclé province, Panama (80°38′W, 8°41′N), and the white-collared manakin was collected on the edge of the Sixaola River and Las Tablas village, Bocas del Toro Province, Panama (82°44′W, 9°32′N). Wet specimens were preserved in 10% neutral buffered formalin. All appropriate governmental agencies including the Smithsonian Tropical Research Institute (STRI), Autoridad Nacional del Ambiente and the Autoridad del Canal de Panama, and University Institutional Animal Care and Use Committees (IACUCs) approved of the collection of specimens for preservation.

Micro-CT Scanning

Our main analysis involved micro-CT scans of the manakins and cotinga. Similar to previous work in this field, we sampled one individual per species (Bostwick et al., 2012; Bird et al., 2014; Van Valkenburgh et al., 2004; Eastman et al., 2014; Crumpton et al., 2015; Piras et al., 2015; Qu et al., 2015; Sentoku et al., 2015; Sharp, 2015). Scans were performed in a General Electric Phoenix Nanotom S Nano-CT scanner. We used Mimics (v. 17.0, Materialise, Leuven, Belgium) software to construct a 3D-model of each species' wing skeleton. The humerus, ulna, and radius were then (graphically) disarticulated, so that measurements could be collected for each tissue. All measurements were recorded and calculated using methods outlined previously by Bostwick et al. (2012). The original scans that we used for our study are currently deposited in an online data repository (Dryad Digital Repository, doi:10.5061/dryad.278q9; http://dx.doi.org/10.5061/dryad.278q9).

Bone Shape

We recorded images of each bone's cross-section at 5% intervals along the long axis. For each measurement, we oriented bones with their greatest length perpendicular to the cross-section view. To adjust for different body sizes among species, we used cross-sections at percentage intervals, as opposed to absolute distance measures. In ImageJ (v 1.49), we measured the longest cross-sectional diameter for each image. We then measured the width of the bone at the midpoint of this long axis. Bone shape at a given cross-section was therefore quantified by dividing the long axis measurement by the width. Measurements of 1.0 indicate the bone is perfectly cylindrical, whereas values greater than 1.0 indicate an oblate (flattened) bone (greater numbers equate to more flattening). Overall, this measurement provides the most suitable estimation of bone shape. Although slight 'twisting' of the bone may change the orientation of the longest bone width, our goal is to determine the general shape, not the orientation of the shape in a particular direction.

Relative Bone Volume

We used Mimics to calculate the relative total volume of each bone, with all foramina capped. To adjust for body size differences among birds, and thus render measurements that were comparable, we divided the cube root of total bone volume by total bone length. The cube root of total bone volume is used because it provides a measure of dimensionality that is comparable to the (linear) measure of length (mm).

Relative Bone Solidness

We used Mimics to calculate the total solidness of each bone (i.e., how much of the structure was filled with bone). This metric was computed by dividing the total volume of ossified bone by the total relative bone volume (see above). We determined total ossified volume using a threshold density determined for each bone scan. It was unnecessary to include a known standard in our scans, as we were more interested in comparisons of relative levels of solidness within or among bones rather than absolute bone density.

We also determined the solidness of each bone at the different cross-sectional slices (see above). In this case, we calculated solidness by dividing the total ossified bone within the cross section by the total volume of the bone within the cross section.

Allometric Analyses

We regressed total bone volume (cube root of ml, see above) on bone length (mm) to assess how these two measures scaled to each other, and whether such scaling differed among bones. Regression models for each bone across all taxa were compared in Prism (v. 4.0) using methods outlined by Zar (1999), and significant effects were followed by Tukey post-hoc comparisons.

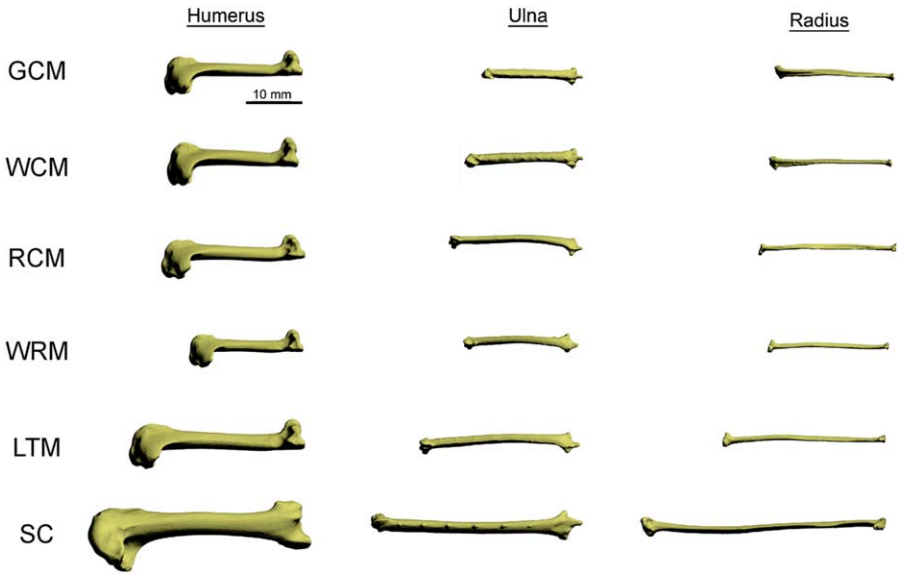

Fig. 1. Three-dimensional renderings of the humerus, ulna, and radius in the six species included in our study. All bones are sized to the same scale. Species names are shown left in the figure. GCM = golden-collared manakin (*Manacus vitellinus*), WCM = white-crowned manakin (*Manacus candei*), RCM = red-capped manakin (*Ceratopipra mentalis*), WRM = white-ruffed manakin (*Corapipo altera*), LTM = lance-tailed manakin (*Chiroxiphia lanceolata*), SC = spangled cotinga (*Cotinga cayana*). [Color figure can be viewed in the online issue, which is available at wileyonlinelibrary.com.]

Wet Specimen Measurements

To validate the main important findings from our micro-CT analysis, we examined golden-collared manakin ($n = 3$), red-capped manakin ($n = 3$), ochre-bellied flycatcher ($n = 3$), and Say's phoebe ($n = 1$) specimens to collect additional morphological measurements, including both radius shape and solidness.

First, we assessed radius shape by calculating eccentricity scores (i.e., collecting longest and shortest shaft diameter; see above) at the 25% and 75% intervals along the bone's long axis (relative to the proximal end). Measurements were taken with calipers (to 0.01mm accuracy). Eccentricity scores were compared using a mixed-effect ANOVA, with species as the between-subjects factor and percent along the bone's long axis as the within-subjects factor (Zar, 1999). Significant main effects and/or interactions were followed with post-hoc comparisons, using Bonferroni corrections.

Second, we assessed radius solidness at the same 75% point along the bone's long axis (relative to the proximal end). We used a razor to cut the bone perpendicularly and then visually scored whether the bone's cross-section was completely solidified or showed at least some form of hollowness. The proportion of solidified vs. hollow bone was compared across species using a Fisher Exact Test modified for a 3×2 design (Freeman and Halton, 1951).

RESULTS

Bone Shape

The three major wing bones for each of the six species used in our study are displayed in Figure 1 (enlarged version of the bones are included in Supporting Information, Figs. S1–S3). Both the humerus and ulna of all taxa are nearly circular across the entire length of the diaphyses (Fig. 2A,B). However, the radius shows species differences in shape; namely, its distal shaft is oblate (flat) in the golden-collared and white-collared manakins, compared to the more circular distal shaft in the other four species (Fig. 2C). The red-capped manakin (*Ceratopipra*) does not have the same morphologically derived radius (Fig. 2D), even though this bird produces mechanical sonations with its wings; notably, however, the red-capped manakin's wing-snaps are kinematically distinct from those of the two species of *Manacus*. Similarly, the lance-tailed manakin (*Chiroxiphia*) and the white-ruffed manakin (*Corapipo*), which also produce limited wing sonations, have no apparent derived specializations of the radius (Figs. 1 and 2C). These results therefore suggest that the flattening of the radius shaft is not a general characteristic of manakins that use their wings to produce sounds. Rather, this unique morphology appears to be specific to the two species of *Manacus* with wings that collide overhead to produce sonations.

Analyses with additional wet specimens of select species supported this finding (Fig. 3). Overall, flatness of the shaft varied among species in our statistical model ($F_{1,6} = 9.61$, $P = 0.013$), with post-hoc tests showing that the golden-collared manakin shaft is significantly flatter than that of both the red-capped manakin ($P = 0.018$) and the ochre-bellied flycatcher ($P = 0.048$). Moreover, measures of flatness between these latter two species were statistically indistinguishable ($P = 1.0$). This model also showed a species × bone region interaction ($F_{1,6} = 8.33$, $P = 0.019$), which indicates that regional differences in radii flatness are species-specific. A analysis of this interaction shows that, in golden-collared manakins, the distal shaft is significantly flatter than the proximal shaft ($P = 0.003$). Such regional differences are not

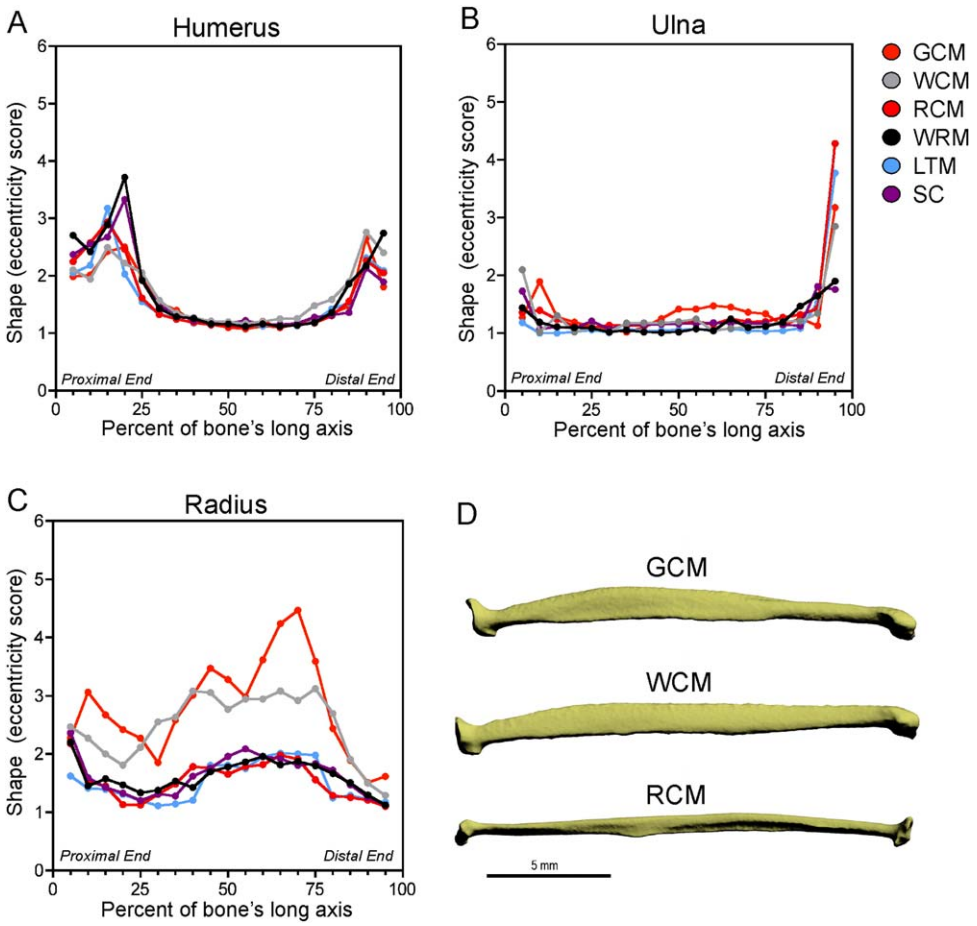

Fig. 2. Cross-sectional shape along the entire long axis of the forelimb bones. (A–C) Shape describes the eccentricity of the cross-sectional diameters, with a value of 1.0 representing perfectly round and numbers greater than 1.0 representing increasing flattening of the bone. The horizontal axis represents the position along the bone, as a percentage of the total length of the bone (see Methods). (D) Radii of representative manakins. GCM and WCM produce percussive, behind-the-back wing-snaps, and thus have flattened radii, whereas RCM produces wing sonations through other mechanisms and thus does not have a flattened radius. Abbreviations as in Figure 1.

present in red-capped manakins ($P = 0.48$) or ochre-bellied flycatchers ($P = 0.28$).

We also collected shape measurements from the same points along the radius shaft of a Say's phoebe specimen, a subosine passerine distantly related to the manakins. Because we obtained only one specimen sample, we did not include this species in our statistical model. However, it is apparent from Figure 3 that the shape of the radius shaft in the Say's phoebe is more circular, and thus closely resembles the radius of the ochre-bellied flycatcher and red-capped manakin.

Relative Bone Volume

For each forearm bone, the total bone volume is similar across taxa (Fig. 4A). The main exception appears to be the spangled cotinga, which has a humerus and ulna with a greater relative volume, compared to the manakins.

Allometric analyses suggest that regression slopes for relative volume versus length are below 1.0 (Table 2). This result implies that bone volume and bird size (as measured by bone length) are negatively allometric, such that wing bones appear to become longer and less voluminous as species evolve increased body size. When we compare allometric relationships among the three wing bones, we find that the humerus is the closest to isometry, followed by the ulna, and then finally the radius (Fig. 4B). Statistical analyses confirm these relationships by showing regression slopes that characterize each bone's scaling between volume and length as significantly different from each other ($F_{2,17} = 49.41$, $P < 0.001$). Indeed, the slope describing humerus scaling is steeper than that of the ulna ($q = 9.56$, $P < 0.001$) and the radius ($q = 13.71$, $P < 0.001$). Moreover, the slope describing the ulna's scaling is steeper than that of the radius ($q = 4.15$, $P < 0.05$). These results should be interpreted cautiously, considering the low sample size in our allometric analyses. Nonetheless, our current findings imply that the humerus

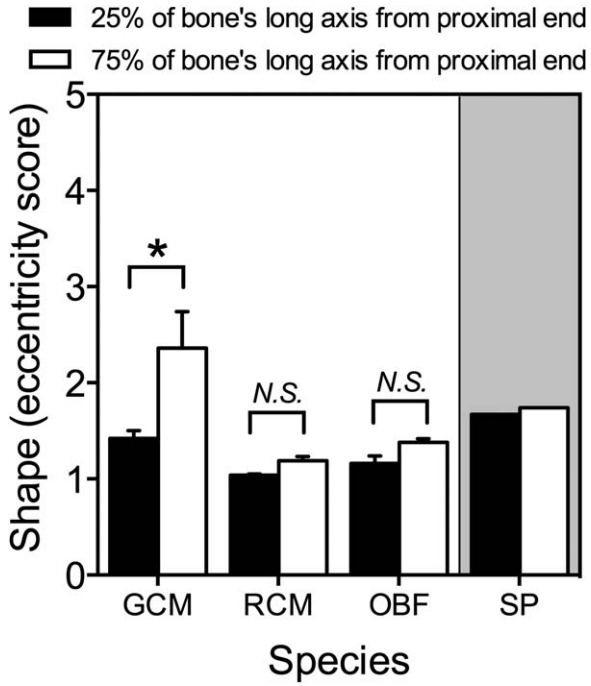

Fig. 3. Shape measurements collected from multiple individuals ($n = 3$ per species) in a subset of species. Shape is represented as the eccentricity scores taken from 25% and 75% intervals along the bones long axis (see Methods). Data represent means ± 1 SEM, with asterisks (*) denoting significant differences in shape between regions of the bone ($P < 0.05$) and 'N.S' denoting no significant difference ($P > 0.05$). Note that the shape of the radius in golden-collared manakin (GCM) is more variable than that of the other two species, and much of this variation occurs at the distal shaft of the radius. Also note that the Say's phoebe (SP) is included in the graph, though its shape measurements were not incorporated into our statistical model because they are from one individual. Abbreviations as in Figure 1.

maintains the strongest scaling effect between volume and size, relative to the ulna and radius. This idea is supported by work evaluating humeral function that posits that larger birds have increased force placed on their forearms during flight, and thus have evolved a more robust humerus to withstand these effects (Biewener, 1982; Cubo and Casinos, 1998). In line with this thinking, our current data are consistent with the notion that the radius is under the least allometric constraint of the three main forearm bones.

Bone Solidness

Total solidness of each forearm bone is also similar across taxa (Fig. 5A). The radius is the most solid of the bones, followed by the ulna, and lastly the humerus.

When examining solidness of bone cross-section, the humerus and ulna are similar among species (Fig. 5B,C). The one notable exception is the white-ruffed manakin, which appears to have a humerus and ulna that are more solidified than the other taxa. This is especially true along both bones' central shafts; otherwise, the solidness of these two bones is generally conserved among the taxa.

These analyses also show that solidification of the radius is unique in both *Manacus*, in that the bone is generally solidified. This effect is most pronounced along the distal end of the shaft, where the entire bone appears to be solid (Fig. 5D). Notably, between the two species of *Manacus*, the radius of the golden-collared manakin appears to be relatively more solid than the radius of the white-collared manakin.

Further analyses of wet specimens confirmed our findings in the radius. That is, all of the golden-collared manakins we examined showed a completely solidified radius at the 75% interval along the bone's long axis (relative to the proximal end). By contrast, both the red-capped manakin and ochre-bellied flycatcher showed hollow bones at this same interval. This proportion of individuals that show solid or hollow radii was significantly different among species (Fisher's Exact test, $P = 0.012$).

DISCUSSION

Our results provide insight into how interactions between evolutionary forces, including natural and sexual selection, likely influence skeletal design in birds. Whereas our results show striking conservation in the volume, shape, and solidness of each wing bone, we also find that the radius in the two M*anacus* is highly derived. Namely, in these congeners, we discover that the distal shaft of the radius is uniquely flattened and 100% solid. Previous work anecdotally reports this morphology and suggests that it supports the production of wing-snap sonations used for courtship and male-male competition (Friscia and Schlinger, 2012; Bodony et al., in press). If so, then this trait is likely sexually selected.

Equally as important, we find that the overall volume and solidness of the radius is indistinguishable among species, including the two species of *Manacus*. We suspect that this is a result of strong natural selection, which undoubtedly favors osteological efficiency to sustain flight by preventing the radius from becoming too large and/or too heavy. Thus, our results collectively suggest that sexual selection alters the radius to facilitate the performance of reproductive displays, but does so within a framework imposed by selective forces that maintain powered flight. This means that features of the radius are likely adjusted in a compartmentalized manner to support the production of behavioral displays that enhance reproductive success, while maintaining basic locomotory function necessary for every-day survival.

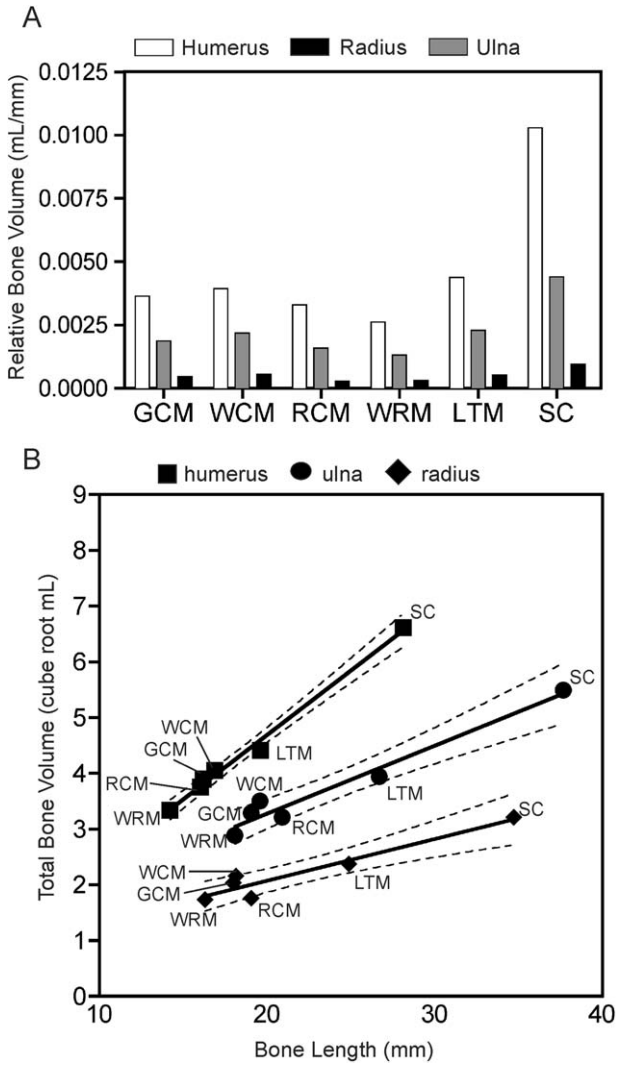

Fig. 4. Relative Bone Volume. (A) Relative bone volume of each forelimb bone for each taxon, as volume (in ml) over length (in mm). (B) Regressions of forelimb bone volume (in cube root ml) versus bone length (in mm). Note that the cube root of the volume was used specifically to investigate allometric scaling because this transformation allows for comparison of measures that are a similar linear dimensionality. Abbreviations as in Figure 1.

Evolution of a Modified Radius

Past work by Bostwick et al. (2012) similarly hinted that sexual selection shapes bone morphology by showing that the club-winged manakin, which performs a complex wing display, maintains a nearly solid ulna (notably, a different forearm bone than the derived radius we uncover herein). This past study, however, neither pinpointed the functional significance of this derived ulna, nor examined whether a congener with a similar display maintains the same derived ulna morphology. Our current study overcomes these issues in two ways. First, we know from prior modeling and anatomical work that *Manacus* hit their wings together above their heads to produce display sonations. The strike initiates at the wrists, and then proceeds proximally, along the radius; thus, the flat, solid shaft of the radius likely assists sound production (Friscia and Schlinger, 2012; Bodony et al., in press). The osteological trait we have uncovered likely supports this impact, and helps generate the ensuing loud, mechanical snap. Second, we show that the flattened, solidified radius is present in two congeners within the genus *Manacus*: golden-collared manakins (*Manacus vitellinus*) and white-collared manakins (*Manacus candei*). All species in this genus produce wing-snaps (Prum, 1990, 1998; Bostwick and Prum, 2003; Fusani et al., 2007), and selection has presumably favored similar radial morphology in other members of this genus to help facilitate this display feature. Consequently, we expect that the unique radius that we discovered is a true adaptation of skeletal morphology to guide display production.

TABLE 2. Regression slopes for allometric relationships between bone length (proxy for body size) and relative bone volume of the species listed in Table 1.

	Regression Metrics			
Bone	Slope	Intercept	R^2	P value
Humerus	0.23125	0.6461	0.9905	<0.001
Ulna	0.12223	0.83012	0.9497	<0.001
Radius	0.07489	0.57875	0.8911	<0.001

Building on this idea, it is interesting that the two *Manacus* species we examined show slight differences in the degree of flattening and solidness of their radii; yet, both species produce robust wing-snaps. This effect may be borne out of differential costs associated with the modified bone. For example, because white-collared manakins inhabit denser forest than golden-collared manakins (McDonald et al., 2001; Uy and Stein, 2007), the flight environments of these two species undoubtedly differ. Diminished structural strength may therefore impact white-collared manakins more severely than their congener, which results in a relaxation of positive selection for a flat and solid radius. To fully address this idea, we would need to examine 3D-reconstructions of the wing skeleton from multiple individuals of each species. Of course other factors, including drift, may explain these differences.

Moreover, we observe no obvious modifications of wing bone morphology in red-capped, white-ruffed, or lance-tailed manakins. Males of these species produce sonations through wing movement, though none of them does so by hitting their wings together (Prum, 1998; Rosselli et al., 2002; Bostwick and Prum, 2003; DuVal, 2007). Red-capped manakins, for example, generate snaps by hitting or rubbing their wings against their bodies, and lance-tailed manakins produce a low-amplitude wing-click during a slow flight phase of their display. During rapid display flights, the

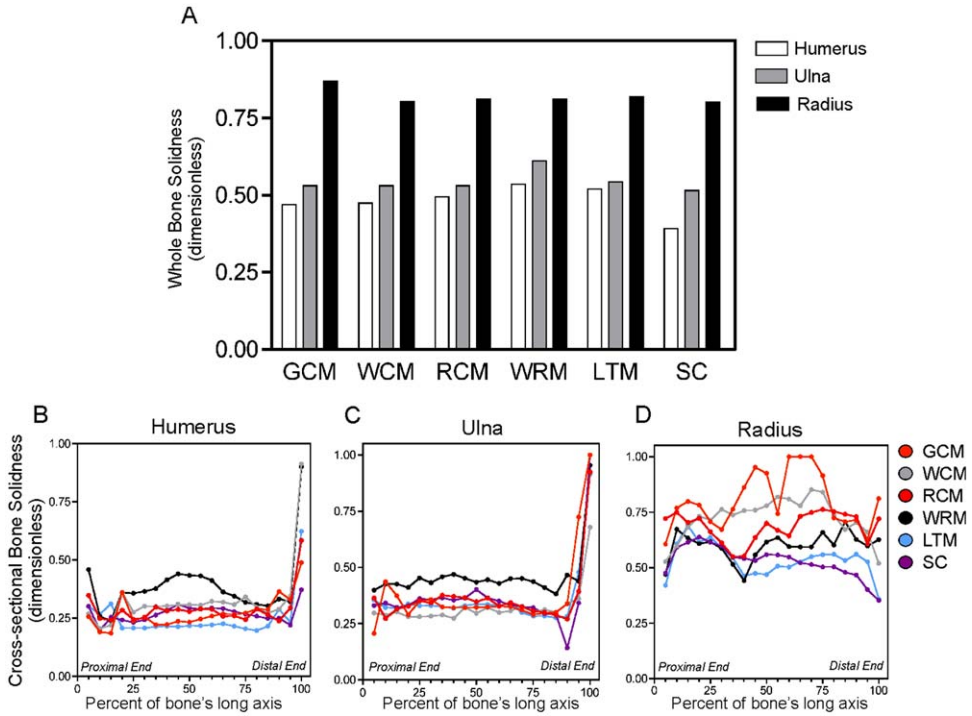

Fig. 5. Bone Solidness. (A) Total bone solidness of each forelimb bone for each taxon, as ossified volume over total bone volume. Values equaling 1.0 represent total solidification, whereas values closer to 0 represent less solidification. (B–D) Bone solidness along the length of each forelimb bone. The horizontal axis represents the position along the bone, as a percentage of the total length of the bone (see Methods). Abbreviations as in Figure 1.

white-ruffed manakin produces a single-pulse non-vocal snap or flop sound, which is thought to be produced from modified feathers (Prum, 1998). Thus, we suspect that the flattened, solidified radius in *Manacus* is not the result of selection for wing sonations in general, given that the ability to produce mechanical sonations has arisen in numerous species that do not show similar radii modification. Instead, this osteological trait is unique to *Manacus*, which hit their wings together (Bostwick and Prum, 2003; Fusani et al., 2007).

Absent from our analysis is an assessment of the club-winged manakin's radius. This species may also show morphological adaptation of the radius, given that they use their wings for extreme physical displays. Bostwick et al. (2012) examined only the ulna and humerus, which makes this comparison impossible. Nonetheless, our work together suggests that bone morphology, in at least the piprids, may be fairly labile to accommodate the family's evolution of elaborate physical displays.

Modification of the Humerus and Ulna

We also uncover a slight modification in morphology of the white-ruffed manakin's humerus and ulna. These two bones are more solidified along their shafts than those of the other species; however, their total solidness is similar across taxa. This again suggests that the solidness of any given part of the bone can be changed within a relatively conserved framework, likely imposed by natural selection. At the same time, we find no evidence that the volume and shape of these bones in white-ruffed manakins differs at all from those of the other birds. Thus, if this species' humerus and ulna are adapted, this has occurred independently of altering the geometric structure of the bones themselves.

Functionally, we speculate that a more solidified humerus (and possibly ulna) contributes to the dramatic aerial displays that white-ruffed manakins produce. In particular, males perform a move (i.e., the *flap-chee-wah*) in which they rapidly fly upwards in a spiral at nearly a vertical angle, before plummeting back down to the forest floor (Rosselli et al., 2002). The force generation required to accelerate vertically in this manner could presumably place excess strain on the humerus (but see Biewener and Dial, 1995). Increased solidification of the humerus shaft may provide additional structural support to help underlie the performance of this display. Of course, the white-ruffed manakin also produces other display maneuvers, including butterfly flights and undulating flights. However, we expect that these do not require the evolution of an especially solidified humerus, because the lance-tailed manakin performs somewhat similar display elements (DuVal, 2007) and does not exhibit the same increased ossified thickness of the main forearm bone.

Putative Costs of Altered Wing Skeletons

The cost associated with the specialized forearm bones raises some interesting questions. This is especially true with respect to the highly derived radius, as bone shape is a primary means by which birds achieve the stiffness and strength to maintain loads during flight (Dumont, 2010). Long bones that are generally hollow and circular, for example, tend to resist torsion better than bones that are relatively more solid and elliptical. Thus, by favoring radii that have regions in which the shaft is highly elliptical and solid, sexual selection likely diminishes flying ability at some level. This represents a putative cost to locomotion that accompanies the emergence of the species' wing-snap behavior. To our knowledge, little anatomical, physiological, and behavioral work has examined such costs in species that perform elaborate physical displays, though speculation that they exist has certainly been mounted (Schlinger et al., 2013; Fusani et al., 2014).

However, given that wing-snap ability has evolved within the genus *Manacus* and that manakins are reasonably strong fliers (Moore et al., 2008), these species obviously cope with structural costs associated with the evolution of their display behavior. Our allometric data provides insight into how this might occur. In effect, relationships between body size and bone volume appear to be strongest with respect to the humerus, which makes sense, given that this bone bears the greatest strain imposed on the forelimbs during flight (Biewener and Dial, 1995; Cubo and Casinos, 1998). At the same time, the relationship between body size and bone volume and solidness appears to be weakest in the radius. This finding is consistent with the idea that radial morphology is relatively less constrained by allometry. If true, this result would imply that the radius is freer to evolve varied morphologies that support non-flight behavior, such as display maneuvering. Further allometric analyses with greater sample size would help bolster this hypothesis; nonetheless, our data currently point to a mechanism by which sexual selection can modify skeletal design to help maximize reproduction, without imposing excessive costs to flight.

In line with this view is the observation that the radii of females of the genus *Manacus* are also flattened (Friscia, pers. obs.). An extensive analysis of sexual dimorphism in bone structure is beyond the scope of this study; however, we note that lack of strong sexual dimorphism in the *Manacus* radius may speak to broader developmental constraints within the avian skeletal design, wherein the sexual selection for the flattened radius in males is carried over to females (Lande, 1980). To this end, costs associated with this trait may be present, but also may not be robust enough to fully extinguish the trait from females. Future work will investigate this issue in *Manacus*.

CONCLUSION

Morphology is often the result of different selective forces, including functional adaptations, allometric scaling, and sexual selection. This is exemplified in the forelimb bones of manakins, specifically species in the genus *Manacus*. Their complex sexual displays have put a selective pressure on the shape of their radii, making them broad and flat along their shaft. This is the first study to investigate this relationship in birds, and it opens up possibilities for investigating similar relationships in other taxa with complex sexual displays.

ACKNOWLEDGEMENTS

We thank A. Tripati, R. Eagle, E. Schuppe, and D. Birds for help using the micro-CT and technical assistance with data collection and interpretation. We thank Joel Stitzel for allowing us to use Mimics software. We thank K. Garret at the Los Angeles Museum of Natural History for providing the cotinga and phoebe specimens, as well as B. Van Valkenburgh for providing valuable insight into this manuscript. We also thank STRI and its administrative staff for their assistance with this project as well as Autoridad Nacional del Ambiente and the Autoridad del Canal de Panama for permission to conduct these studies. This work was funded by intramural start-up funds from Wake Forest University (to M.J.F.).

LITERATURE CITED

Barske J, Fusani L, Wikelski M, Feng NY, Santos M, Schlinger BA. 2014. Energetics of the acrobatic courtship in male golden-collared manakins (*Manacus vitellinus*). Proc R Soc B 281:20132482-

Barske J, Schlinger BA, Wikelski M, Fusani L. 2011. Female choice for male motor skills. Proc R Soc B 278:3523–3528.

Beehler B, Pruett-Jones SG. 1983. Display dispersion and diet of birds of paradise: a comparison of nine species. Behav Ecol Sociobiol 13:229–238.

Biewener AA. 1982. Bone strength in small mammals and bipedal birds: do safety factors change with body size? J Exp Biol 98:289–301.

Biewener AA, Dial KP. 1995. In vivo strain in the humerus of pigeons (*Columbia livia*) during flight. J Morphol 225:61–75.

Bird DJ, Amirkhanian A, Pang B, Van Valkenburgh B. 2014. Quantifying the cribriform plate: influences of allometry, function, and phylogeny in Carnivora. Anat Rec 297:2080–2092.

Bostwick KS, Prum RO. 2003. High-speed video analysis of wing-snapping in two manakin clades (Pipridae: Aves). J Exp Biol 206:3693–3706.

Bostwick KS, Riccio ML, Humphries JM. 2012. Massive, solidified bone in the wing of a volant courting bird. Biol Lett 8: 760–763.

Bodony DJ, Day L, Friscia AR, Fusani L, Kharon A, Swenson GW, Jr, Wikelski M, Schlinger BA. 2016. Determination of the wingsnap sonation mechanism of the Golden-collared manakin (Manacus vitellinus). J Exp Biol. doi: 10.1242/jeb.128231.

Chaves L. 2001. Observations on diet, foraging behaviour, vocalisations and displays of spangled cotinga, *Cotinga cayana*. Cotinga 16:101–102.

Clifton GT, Hedrick TL, Biewener AA. 2015. Western and Clark's grebes use novel strategies for running on water. J Exp Biol 218:1235–1243.
Crumpton N, Kardjilov N, Asher RJ. 2015. Convergence vs. Specialization in the ear region of moles (mammalia). J Morphol 276:900–914.
Cubo J, Casinos A. 1998. The variation in cross-sectional shape in the long bones of birds and mammals. Annal Sci Naturelles 1:51–62.
Currey JD, Alexander RM. 1985. The thickness of the walls of tubular bones. J Zool 206:453–468. (AUG):
Dumont ER. 2010. Bone density and the lightweight skeletons of birds. Proc R Soc B 277:2193–2198.
DuVal EH. 2007. Cooperative display and lekking behavior of the lance-tailed manakin (*Chiroxiphia lanceolata*). Auk 124: 1168–1185.
Eastman JT, Witmer LM, Ridgely RC, Kuhn KL. 2014. Divergence in skeletal mass and bone morphology in antarctic notothenioid fishes. J Morphol 275:841–861.
Fedducia A. 1996. The origin and evolution of birds. New Haven: Yale University Press.
Freeman GH, Halton JH. 1951. Note on the exact treatment of contingency, goodness of fit and other problems of significance. Biometrika 38:141–149.
Friscia AR, Schlinger BA. 2012. Unique wing morphology in wing-snapping Manacus manakins. Integr Comp Biol 52:e61
Fusani L, Barske J, Day LD, Fuxjager MJ, Schlinger BA. 2014. Physiological control of elaborate male courtship: female choice for neuromuscular systems. Neurosci Biobehav Rev 46:534–546.
Fusani L, Giordano M, Day LB, Schlinger BA. 2007. High-speed video analysis reveals individual variability in the courtship displays of male golden-collared manakins. Ethology 113:964–972.
Fuxjager MJ, Longpre KM, Chew JG, Fusani L, Schlinger BA. 2013. Peripheral androgen receptors sustain the acrobatics and fine motor skill of elaborate male courtship. Endocrinology 154:3168–3177.
Gill FB. 2007. Ornithology. New York: Freeman & Co.
Habib MB, Ruff CB. 2008. The effects of locomotion on the structural characteristics of avian limb bones. Zool J Linn Soc 153:601–624.
Hone DWE, Naish D, Cuthill IC. 2011. Does mutual sexual selection explain the evolution of head crests in pterosaurs and dinosaurs. Lethaia 45:139–156.
Jaramillo A, Burke P. 1999. New World Blackbirds: The Icterids. Princeton: Princeton University Press.
Lande R. 1980. Sexual dimorphism, sexual selection, and adaptation in polygenic characters. Evolution 34:292–305.
McDonald DB, Clay RP, Brumfield RT, Braun MJ. 2001. Sexual selection on plumage and behavior in an avian hybrid zone: Experimental tests of male-male interactions. Evolution 55: 1443–1451.
Moore RP, Robinson WD, Lovette IJ, Robinson TR. 2008. Experimental evidence for extreme dispersal limitation in tropical forest birds. Ecol Lett 11:960–968.
Naish D, Perron R. 2014. Structure and function of the cassowary's casque and its implications for cassowary history, biology and evolution. Hist Biol 1–12.
Olson VA, Turvey ST. 2013. The evolution of sexual dimorphism in New Zealand giant moa (Dinornis) and other ratites. Proc R Soc B 280:20130401
Piras P, Sansalone G, Teresi L, Moscato M, Profico A, Eng R, Cox TC, Loy A, Colangelo P, Kotsakis T. 2015. Digging adaptation in insectivorous subterranean eutherians. The enigma of Mesoscalops montanensis unveiled by geometric morphometrics and finite element analysis. J Morphol 276:1157–1171.
Prum RO. 1990. Phylogenetic analysis of the evolution of display behavior in the neotropical manakins (Aves, Pipridae). Ethology 84:202–231.
Prum RO. 1998. Sexual selection and the evolution of mechanical sound production in manakins (Aves: Pipridae). Anim Behav 55:977–994.
Qu Q, Blom H, Sanchez S, Ahlberg P. 2015. Three-dimensional virtual histology of silurian osteostracan scales revealed by synchrotron radiation microtomography. J Morphol 276: 873–888.
Rosselli L, Vasquez P, Ayub I. 2002. The courtship displays and social system of the white-ruffed manakin in Costa Rica. Wilson Bull 114:165–178.
Schlinger BA, Barske J, Day L, Fusani L, Fuxjager MJ. 2013. Hormones and the neuromuscular control of courtship in the golden-collared manakin (*Manacus vitellinus*). Front Neuroendocrinol 34:143–156.
Schlinger BA, Fusani L, Day L. 2008. Hormonal control of courtship in male Golden-collared manakins (*Manacus vitellinus*). Ornitol Neotrop 19:229–239.
Schukman JM, Wolf BO. 1998. Say's phoebe (Sayornis saya). In: Poole A, Gill F, editors. The Birds of North America. Washington D.C.: Academy of Natural Sciences, Philadelphia and American Ornithologists' Union.
Sentoku A, Ishibashi M, Masumoto S, Ohno R, Tomiyama T, Machiyama H, Tadai O, Ezaki Y. 2015. Regular budding modes in a zooxanthellate dendrophylliid Turbinaria peltata (Scleractinia) revealed by X-ray CT imaging and three-dimensional reconstruction. J Morphol 276:1100–1108.
Sharp AC. 2015. Comparative finite element analysis of the cranial performance of four herbivorous marsupials. J Morphol 276:1230–1243.
Uy JAC, Stein AC. 2007. Variable visual habitats may influence the spread of colorful plumage across an avian hybrid zone. J Evol Biol 20:1847–1858.
Van Valkenburgh B, Theodor J, Friscia A, Pollack A, Rowe T. 2004. Respiratory turbinates of canids and felids: a quantitative comparison. J Zool 264:281–293.
Wallace AR. 1869. The Malay Archipelago: The land of the orang-utan, and the bird of paradise. A narrative of travel, with studies of man and nature. New York: Harper & Brothers.
Westcott DA, Smith JNM. 1994. Behavior and social organization during the breeding season in *Mionectes oleagineua*, a lekking flycatcher. Condor 96:672–683.
Weston EM, Friday AE, Lio P. 2007. Biometric evidence that sexual selection has shaped the Hominin face. PLoS One 2:e710
Zar JH. 1999. Biostatistical Analysis. Upper Saddle River: Prentice Hall.